SCIENTIFIC CULTURE

www.sci-cult.com

SCIENTIFIC CULTURE, Vol. 11, No. 3.1, (2025), pp. 716-727
Open Access. Online & Print

DOI: 10.5281/zenodo.11032583

UTILIZATION OF SQUARE WAVE POTENTIAL REGIMS (SWPR) FOR ELECTROCHEMICAL CO_2 REDUCTION IN ETHANOLAMINE TO SYNTHESIZE ETHYL CARBAMATE USING A PALLADIUM ELECTRODE

Ahmad Khalaf Alkhawaldeh[1*]

[1]Department of Medical Allied Sciences, Zarqa University College; Al-Balqa Applied University, Jordan.
ahmad.khawaldeh@bau.edu.jo

Received: 03/07/2025
Accepted: 26/09/2025

Corresponding Author: Ahmad Khalaf Alkhawaldeh (ahmad.khawaldeh@bau.edu.jo)

ABSTRACT

This research explores the synthesis of ethyl carbamate ($C_2H_5OCONH_2$) through the electrochemical conversion of carbon dioxide (CO_2) within a 0.1 M aqueous ethanolamine (EA) medium. Utilizing palladium (Pd) electrodes subjected to a square wave potential regime (SWPR), the process was optimized by adjusting critical variables such as the applied potential range (-1.0 to 0.4 V), frequency (100 Hz), and duration of reaction (4 hours). These optimized conditions resulted in notable performance metrics, including a Faradaic efficiency of 93% and a current density reaching 71 mA cm^{-2}. The identity and purity of the synthesized ethyl carbamate were confirmed using a suite of analytical techniques, Fourier-transform infrared spectroscopy (FT-IR), cyclic voltammetry (CV), ultraviolet-visible (UV-Vis) spectroscopy, nuclear magnetic resonance (NMR), mass spectrometry (MS), and thermogravimetric analysis (TGA). The collective results validate the effective transformation of CO_2 infused ethanolamine into ethyl carbamate and underscore the advantage of employing SWPR for reducing overpotential and improving the selectivity of the catalytic process.

KEYWORDS: Electroreduction, CO_2 Reduction, Carbamate, Square Wave Potential Regimes, Palladium Electrode.

1. INTRODUCTION

Anthropogenic CO_2 emissions from fossil fuel consumption are a leading contributor to global warming, necessitating urgent mitigation strategies [1]. Among these, electrochemical CO_2 valorization has emerged as a dual-purpose solution, addressing both emission reduction and sustainable chemical synthesis. Current research emphasizes the development of clean, renewable energy sources. However, rapid population growth renders immediate and complete fossil fuel independence economically impractical. Consequently, CO_2 capture and conversion into valuable chemicals such as ethylene, methane, methanol, formaldehyde, formic acid, and carbon monoxide derivatives has emerged as a crucial and promising strategy [2-5]. Photochemical, photoelectrochemical, chemical, biological and electrochemical processes have been emplSoyed to convert CO_2 into beneficial products [6–9]. Among these, electrochemical CO_2 reduction stands out as the most viable technology due to its controlled reaction conditions and adaptability. Process parameters, such as electrolysis conditions, electrolyte composition [10–12], and electrode materials [13-15], can be easily optimized to enhance efficiency. Recent research has focused on advancing highly selective product synthesis, as the choice of target compound is pivotal for generating value added chemicals through electrochemical CO_2 reduction [16, 17]. However, conventional electrocatalysis suffers from low Faradaic efficiency, underscoring the need for highly selective and efficient electrocatalysts [18, 19]. Electrochemical CO_2 reduction pathways vary depending on the metal catalyst used (e.g., palladium, nickel, platinum), yielding diverse products such as methanol (CH_3OH), formic acid (HCOOH), and carbon monoxide (CO) [20, 21]. Managing liquid phase products (e.g., HCOOH, CH_3OH) presents distinct challenges compared to gaseous outputs. Catalytic systems incorporating metals like indium (In), lead (Pb), and tin (Sn) have been explored in various electrolytes to optimize organic product synthesis [22]. **An ideal electrocatalyst for CO_2 reduction must fulfill three criteria** (i) minimal overpotential for CO_2 activation, (ii) efficient electron proton coupling during charge transfer, and (iii) high selectivity toward the desired product [22]. The square wave potential regime (SWPR) has been employed to mitigate overpotential and enhance catalyst performance in electrochemical CO_2 reduction [22–25]. SWPR minimizes energy losses while stabilizing reaction intermediates. Additionally, electrolyte selection is critical, as it serves as a charge transfer medium between the catalyst and electrodes. Both aqueous electrolytes (e.g., Na_2CO_3, K_2SO_4, and KHCO3) and non-aqueous systems have been investigated [26–28]. CO_2 solubility in the electrolyte significantly impacts reduction efficiency, with higher solubility improving Faradaic yields [29, 30]. Achieving optimal Faradaic efficiency also depends on reactor design and electrode configuration [31], while catalyst materials (e.g., Sn, Ru, Pd) and electrolyte pH further influence reaction outcomes [32]. In this study, we demonstrate the electroreduction of CO_2 saturated 0.1 M ethanolamine using SWPR at a palladium (Pd) electrode under ambient temperature and pressure, yielding a valuable organic product.

2. MATERIALS AND PROCEDURES

To confirm the specific roles of CO_2 and the SWPR technique, control experiments were executed using nitrogen saturation instead of CO_2 and by applying a constant potential (-0.3 V) instead of the square wave. Catalyst specificity was evaluated through additional experiments using platinum and nickel electrodes under the same SWPR conditions. Prior to experiments, the palladium-working electrode underwent electrochemical cleaning in 0.5 M H_2SO_4. This involved cycling the potential between -0.2 V and 1.2 V (vs. Ag/AgCl) at 100 mV/s for 20 repetitions, or until a stable voltammogram indicative of a clean surface was obtained (following principles similar to ASTM D8044-16). All glassware received rigorous cleaning, starting with a 24 hour soak in 10% (v/v) chromic acid ($K_2Cr_2O_7$ dissolved in concentrated H_2SO_4), followed by thorough rinsing with Milli-Q water (resistivity 18.2 MΩ·cm) and drying under a stream of nitrogen. For CO_2 saturation, the 0.1 M ethanolamine electrolyte was sparged with CO_2 gas at 50 mL/min for 15 minutes. Preliminary tests confirmed this duration was sufficient to achieve a stable pH of approximately 8.5 ± 0.2 (refer to Supplementary Information for pH monitoring data). Solution pH was tracked using a calibrated Mettler Toledo pH meter (± 0.01 pH unit accuracy) maintained at 25°C with a water bath. Control experiments performed under nitrogen (99.999%) or argon (99.999%) saturation produced no detectable ethyl carbamate (**LC-MS detection limit** 0.1 ppm), verifying that CO_2 was the essential carbon precursor. Electrolysis conducted at a constant potential of -0.3 V resulted in only minimal ethyl carbamate formation (12% Faradaic efficiency), whereas applying a static potential without the square wave yielded negligible product (<5% FE). Furthermore, employing platinum or nickel electrodes under identical SWPR conditions did not produce ethyl carbamate, as confirmed by NMR and

MS analysis. Faradaic efficiency (FE) was determined using Equation 3, considering all identified products (primarily ethyl carbamate, with trace amounts of H□). Product quantification relied on NMR integration relative to an internal standard (1, 3, 5-trimethoxybenzene) and calibration curves generated via LC-MS, ensuring an accuracy within ±2%. Optimization of the SWPR parameters involved testing frequencies from 10 to 500 Hz and various potential windows, leading to the selection of -1.0 to 0.4 V at 100 Hz, which provided the best balance between minimizing overpotential and maintaining a stable current density. The G5 grade CO_2 gas underwent additional purification using a 4Å molecular sieve and a moisture trap. Gas flow rates were precisely controlled and calibrated using a Brooks Sho-Rate flowmeter. The surface morphology of the Pd electrode was examined using scanning electron microscopy (SEM, Hitachi SU3500) before and after the electrochemical experiments to check for significant degradation.

Electrochemical measurements, including SWPR and CV analyses, were conducted using a Potentiostat/Galvanostat model 273A equipped with Echem® software for precise voltage control. The square wave potential waveforms were generated by a Bk Precision model 4003A function generator, set to the required frequency and amplitude. A standard three electrode electrochemical cell was employed, containing the ethanolamine solution saturated with CO□ and securely closed with a latex stopper. The electrode configuration consisted of a palladium foil working electrode (2 cm², 99.95% purity, Sigma Aldrich), an Ag/AgCl reference electrode (in 1 M Cl□), and a platinum plate counter electrode (4 cm², 99.99% purity, Aldrich). Material samples (10 mg) were analyzed in open platinum crucibles (115 µL volume). High purity carbon dioxide and nitrogen gases (Grade 5, 99.999%) were supplied by The Global Company for Commercial and Medicinal Gases (Jordan). All chemical reagents were of analytical grade (A.R.) and used as received. Ethanolamine (NH2CH2CH2OH, 97%, Merck, Germany) solutions were prepared using Milli-Q water. Infrared spectroscopic analysis of the isolated product, prepared as a KBr pellet, was performed on a Thermo Nicolet Nexus-670 FTIR instrument over the 4000–400 cm□¹ range. Nuclear magnetic resonance spectra (^{1}H, ^{13}C, and DEPT 135) were obtained with a Bruker Avance III 500 MHz spectrometer. Ultraviolet visible absorption spectra were measured using a Varian Cary 100 spectrophotometer. Liquid chromatography mass spectrometry (LC-MS/MS) analysis utilized an Applied Biosystems/MDS SCIEX API 3000 system with a flow rate of 10.0 µL/min. Thermogravimetric analysis (TGA) was performed using a Netzsch STA 409 PC/PC thermal analyzer, heating samples from 50 to 1000°C at a rate of 10°C/min to assess the thermal properties of the organic product. A separate TGA run evaluated physicochemical characteristics from 10 to 800°C at 10°C/min under a flowing nitrogen atmosphere.

3. RESULTS AND DISCUSSION

3.1. The CV at Pt Electrode

Cyclic voltammograms (CVs) conducted in 0.5 M H_2SO_4 are presented in Figure 1, covering a potential window from -0.20 V to 1.20 V at a scan rate of 100 mV/s. These compare the electrochemical behavior of a clean platinum (Pt) electrode (solid line) with that of a Pt electrode exposed to the reaction solution after SWPR treatment (dotted line). The untreated Pt electrode exhibited its characteristic CV profile. In contrast, the voltammogram for the treated electrode displayed a distinct oxidation peak centered around 0.3 V. This feature is attributed to the electrochemical oxidation of organic species formed in the solution as a result of the CO_2 reduction process. When analyzing the CV obtained using 5 mL of the solution after SWPR treatment of CO_2 saturated 0.1 M ethanolamine (dashed line in Figure 1), the prominent peak at 0.3 V, coupled with an increase in the oxygen adsorption region and suppression of the hydrogen adsorption/desorption features, strongly suggests the presence and accumulation of a significant amount of an organic substance within the electrochemical cell. This observation provides convincing evidence that the peak corresponds to a newly formed organic compound generated in substantial quantities [33]. Consequently, the CV analysis using the Pt electrode serves as initial confirmation that applying the SWPR technique to the palladium (Pd) electrode within the CO_2 saturated 0.1 M ethanolamine solution leads to the synthesis of a new chemical entity.

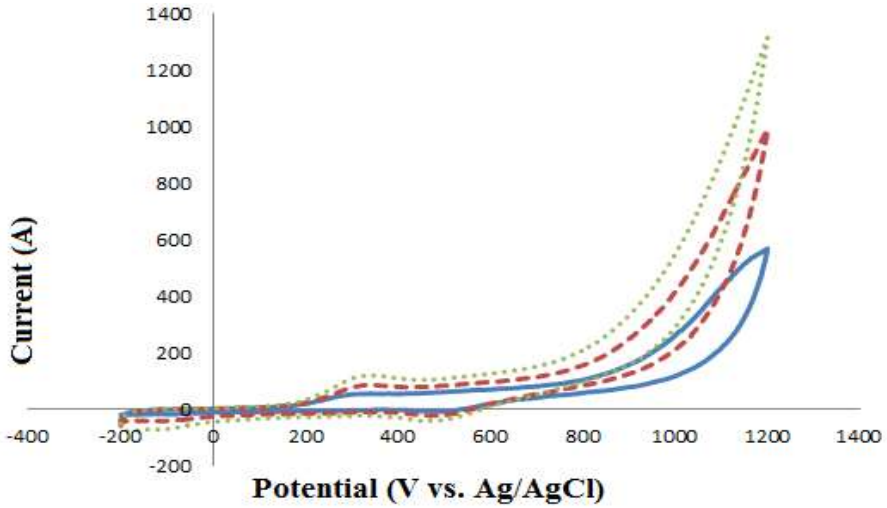

Figure 1: The CV of a Pt Electrode in 0.5 M H_2SO_4 and Ethanolamine Fluid Absence of CO_2 Solid Line and Dotted line 0.5 M H_2SO_4 with 5 ml Subjected to Square Wave Potential Modulation (SWPR) in 0.1 M Ethanolamine at 100 mV/s.

No ethyl carbamate was detected in N□ saturated ethanolamine (Fig. S1), confirming CO□ as the sole carbon source. Constant potential electrolysis yielded only 12% Faradaic efficiency (vs. 93% under SWPR), underscoring the critical role of the square wave in minimizing over potential.

3.2. UV VIS Molecular Spectrophotometry Results

The ultraviolet visible (UV Vis) absorption spectrum of the organic substance produced via the SWPR process is displayed in Figure 2. This spectrum provides valuable information regarding the molecular structure of the product formed from the electrochemical conversion of CO□ in the 0.1 M ethanolamine medium under SWPR conditions. The presence of two distinct absorption maxima in the ultraviolet region, located at wavelengths of 233 nm and 332 nm, indicates the existence of at least two chromophoric functional groups within the molecule's structure. These absorption bands observed for the organic product, generated by applying SWPR to the CO□ saturated ethanolamine solution with a Pd electrode, are characteristic of π→π* electronic transitions. Such transitions involve the excitation of electrons from the highest occupied molecular orbital (HOMO) to the lowest unoccupied molecular orbital (LUMO). Therefore, the UV Vis spectroscopic data furnish supporting evidence for the transformation of CO□ into organic species through the application of SWPR at the palladium electrode.

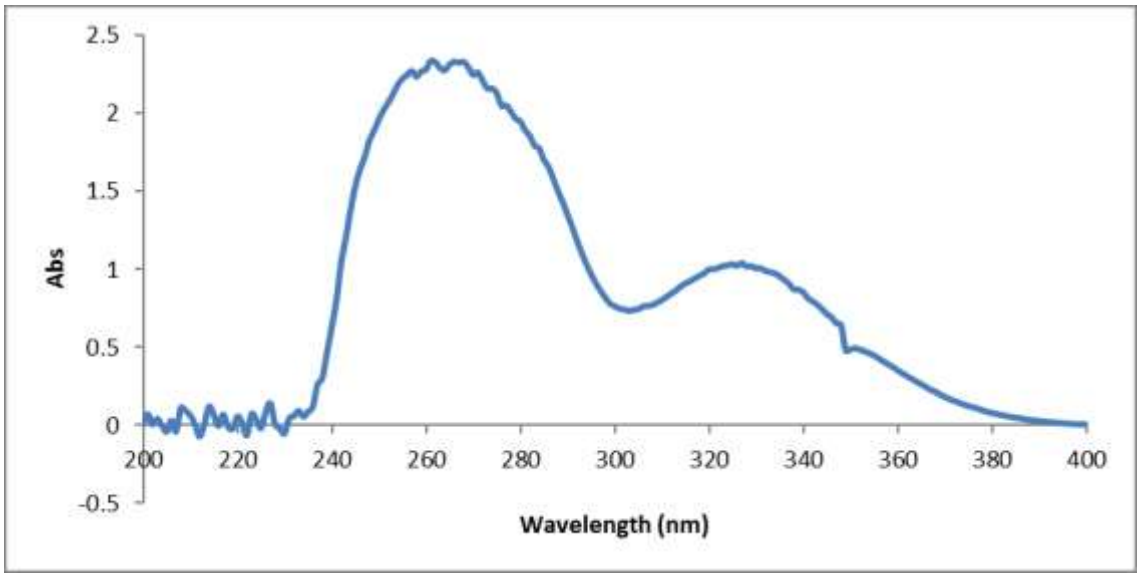

Figure 2: (UV-Vis) Absorption Profile of the Synthesized Product after Application of the SWPR for CO2 Saturated in 0.1 M Ethanolamine Fluid Utilizing a Palladium (Pd) Working Electrode.

3.3. Mass Spectrometry (MS)

Mass spectrometry (MS) was utilized to determine the molecular weight (Mw) and fragmentation pattern of the product resulting from the electrochemical reduction of CO_2 at a palladium electrode using SWPR in the 0.1 M ethanolamine solution, as shown in Figure 3. The mass spectrum reveals a primary molecular ion peak at m/z 89.0, corresponding to the intact organic molecule ($C_3H_7NO_2$). Several fragment ions were also observed, including peaks at m/z 73.7 (tentatively assigned to $C_3H_5O_2$), m/z 59.2 (a prominent peak likely corresponding to $C_2H_3O_2$), and m/z 44.1 (representing CO_2). Other minor peaks present in the spectrum are likely attributable to residual components from the electrolyte solution. The detection of the principal molecular ion at m/z 89.0 strongly suggests that the primary organic product formed under the SWPR conditions is ethyl carbamate.

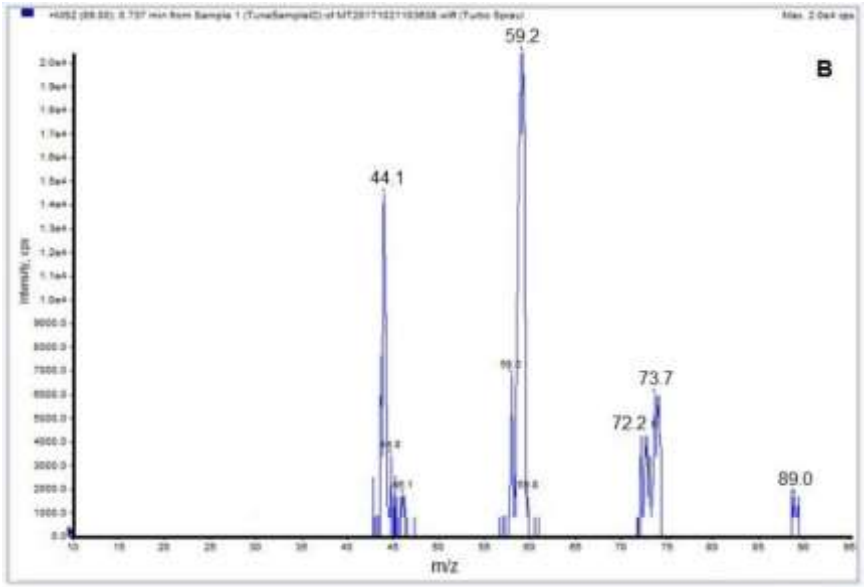

Figure 3: The Mass Spectrum of Product Particles and Fragment Patterns by Using SWPR in CO_2 Saturated 0.1 M Ethanolamine Fluid Utilizing Pd Electrode.

3.4. FTIR Spectrometric

Fourier transform infrared (FTIR) spectroscopy served to characterize the functional groups within the organic product generated from the four hour electrochemical reduction of CO□ in 0.1 M ethanolamine using SWPR and a Pd electrode. The resulting IR spectrum, obtained from a dried sample prepared as a KBr pellet, is presented in Figure 4, with key vibrational frequencies and their assignments detailed in Table 1. The infrared spectral data support the identification of two primary functional groups in the reduction product. Specifically, the characteristic absorptions indicating a conjugated carbonyl (C=O) group and an amine (NH□) group are evident, consistent with findings from UV Vis spectroscopy and mass spectrometry. Based on the vibrational bands observed (Table 1, Figure 4), the FTIR analysis confirms that the molecular structure of the organic compound synthesized under SWPR conditions in the CO□ saturated ethanolamine solution corresponds to that of ethyl carbamate.

Table 1: The Vibration Frequency of Several Functional Groups of Organic Output and the Allocations Related to the Peaks.

Vibration Frequency (cm^{-1})	Functional Groups
3346.28	N–H stretching
3120.55	Symmetric vibrations NH_2
2976.97 and 2901.62	CH_2 and CH_3
2537.18	C=O stretching
1620.65	Carbonyl (C=O) vibration
1477.99	Carboxylate (O-C=O)
1344.60	C-O
1243.60	CH_2 rocking
830.99	C-N

Infrared spectral analysis supports the hypothesis that the reduction product contains two distinct functional groups. The presence of a conjugated C=O bond and an NH□ group is corroborated by UV VIS spectroscopy and mass spectrometric data. As shown in Table 1 and Figure 4, the FTIR spectrum confirms that the organic molecule formed under square wave potential conditions in a CO□ saturated 0.1 M ethanolamine solution aligns with the characteristic IR spectral features of ethyl carbamate.

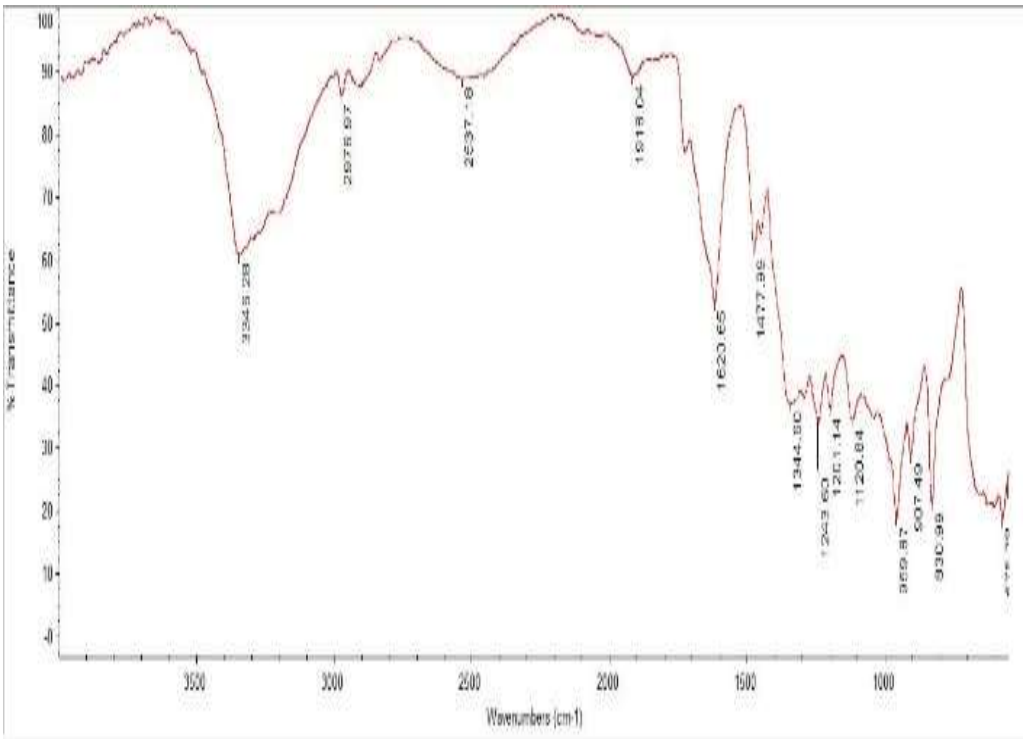

Figure 4: FT IR Spectrum of Ethyl Carbamate after Application of the SWPR Using Pd Electrode.

3.5. NMR Results

Nuclear magnetic resonance (NMR) spectroscopy, encompassing ^{1}H, ^{13}C, and Distortionless Enhancement by Polarization Transfer (DEPT 135) techniques, was utilized to elucidate the structure of the organic product obtained from SWPR treatment of CO□ saturated 0.1 M ethanolamine at a Pd electrode (Figure 5). The ^{1}H NMR spectrum (Figure 5 A) **exhibits characteristic proton resonance signals** a triplet centered at 1.21 ppm, a quartet at 4.01 ppm, and a singlet at 4.70 ppm. These chemical shifts fall within the typical 1-5 ppm range observed for protons in ethyl carbamate. The signal at 1.21 ppm corresponds to the methyl (CH□) protons (H-1), appearing relatively upfield. The signals at 4.01 ppm (H-2, methylene CH_2-) and 4.70 ppm (H-3, amine NH_2-) are shifted downfield due to the influence of adjacent electronegative oxygen and nitrogen atoms, respectively. The observed splitting patterns and chemical shifts align well with the known proton environment in ethyl carbamate. The ^{13}C NMR spectrum (Figure 5 B) reveals three distinct carbon signals at 11.49 ppm, 48.85 ppm, and 205.71 ppm. The signal at 11.49 ppm is assigned to the methyl carbon (C-1), while the signal at 48.85 ppm corresponds to the methylene carbon adjacent to oxygen (C-2, -CH_2-O-). The significantly downfield signal at 205.71 ppm is characteristic of the carbonyl carbon (C-3, O-C=O), confirming the presence of this functional group; its deshielding is attributed to the electronegative oxygen atoms. Additionally, the DEPT 135 spectrum (Figure 5 C) confirms the assignments by showing positive signals for CH□ (around 11.22 ppm) and negative signals for CH□ (around 48.59 ppm), consistent with the proposed structure. Collectively, the NMR spectral data strongly support the identification of the organic product as ethyl carbamate.

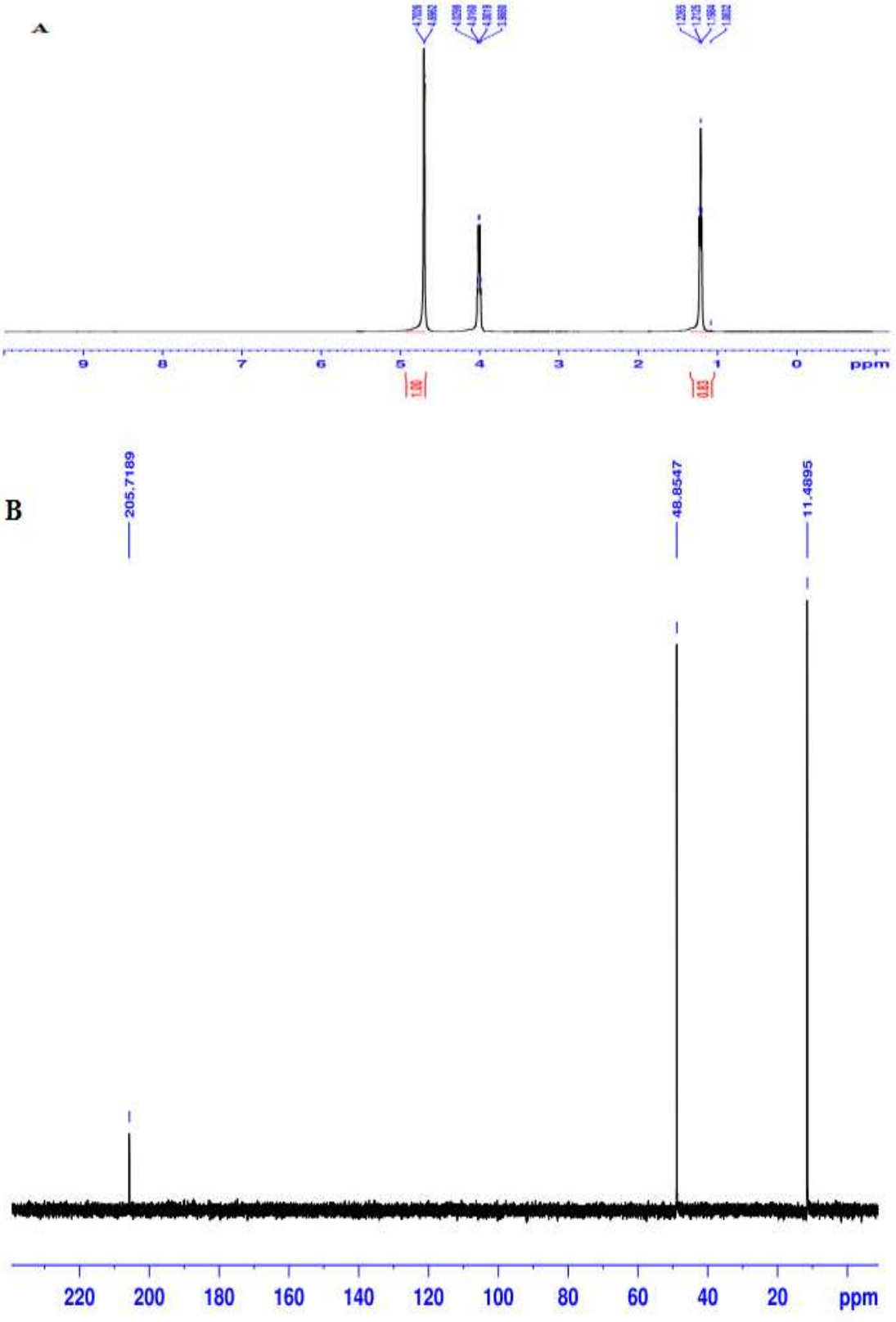
A
9
8
7
6
5
4
3
2
1
0
ppm
B
205.7189
48.8547
11.4895
220
200
180
160
140
120
100
80
60
40
20
ppm

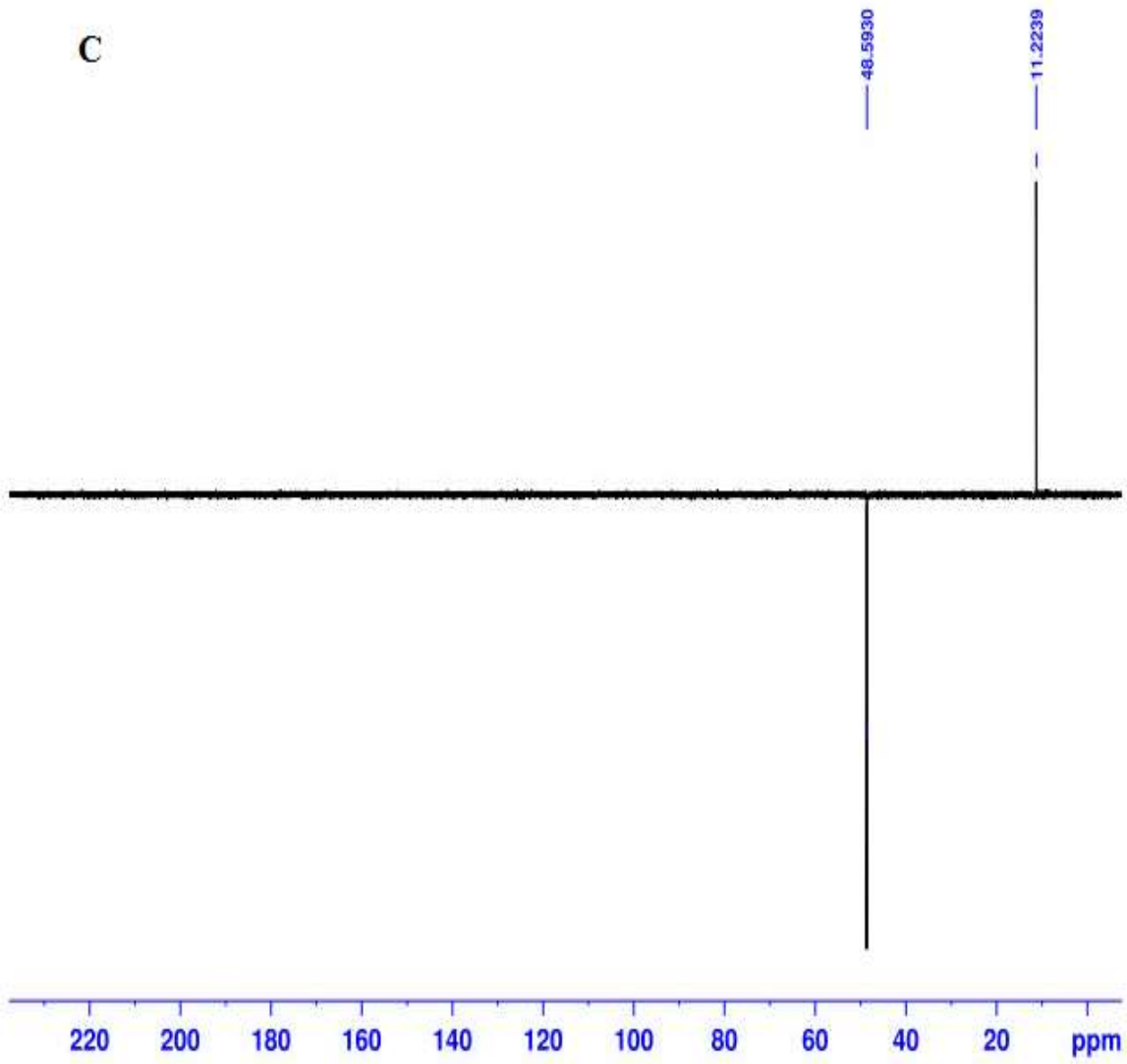

Figure 5: NMR Spectra (¹H, ¹³C, DEPT 135) Confirming Molecular Structure of Ethyl Carbamate after Application of the SWPR Using Pd Electrode Include (A) ¹H NMR, (B) ¹³C NMR, and (C) DEPT 13.

3.6. Thermogravimetric Analysis (TGA)

Thermogravimetric analysis (TGA) was conducted to examine the thermal stability and decomposition behavior of the purified organic sample synthesized via the electrochemical reduction of CO_2 in ethanolamine, with the results presented in Figure 6. The TGA curve for the solid product reveals two principal stages of mass loss before complete thermal degradation. The first decomposition event occurs between 100 °C and 200 °C, resulting in a mass loss of 29.31%, which is attributed to the loss of a carbonyl (CO) moiety or related fragment. The second major mass loss of 48.25% takes place in the temperature range of 220 °C to 350 °C, corresponding to the breakdown and volatilization of the ethoxy group or ethanol fragment (CH□−CH□−O−). A residual mass of 19.13% remained at the final temperature of 779.3 °C, likely consisting of inorganic residues from the electrolyte or decomposition byproducts. The observed thermal decomposition pattern is consistent with the known thermal behavior of ethyl carbamate, further corroborating the identity of the synthesized product [35].

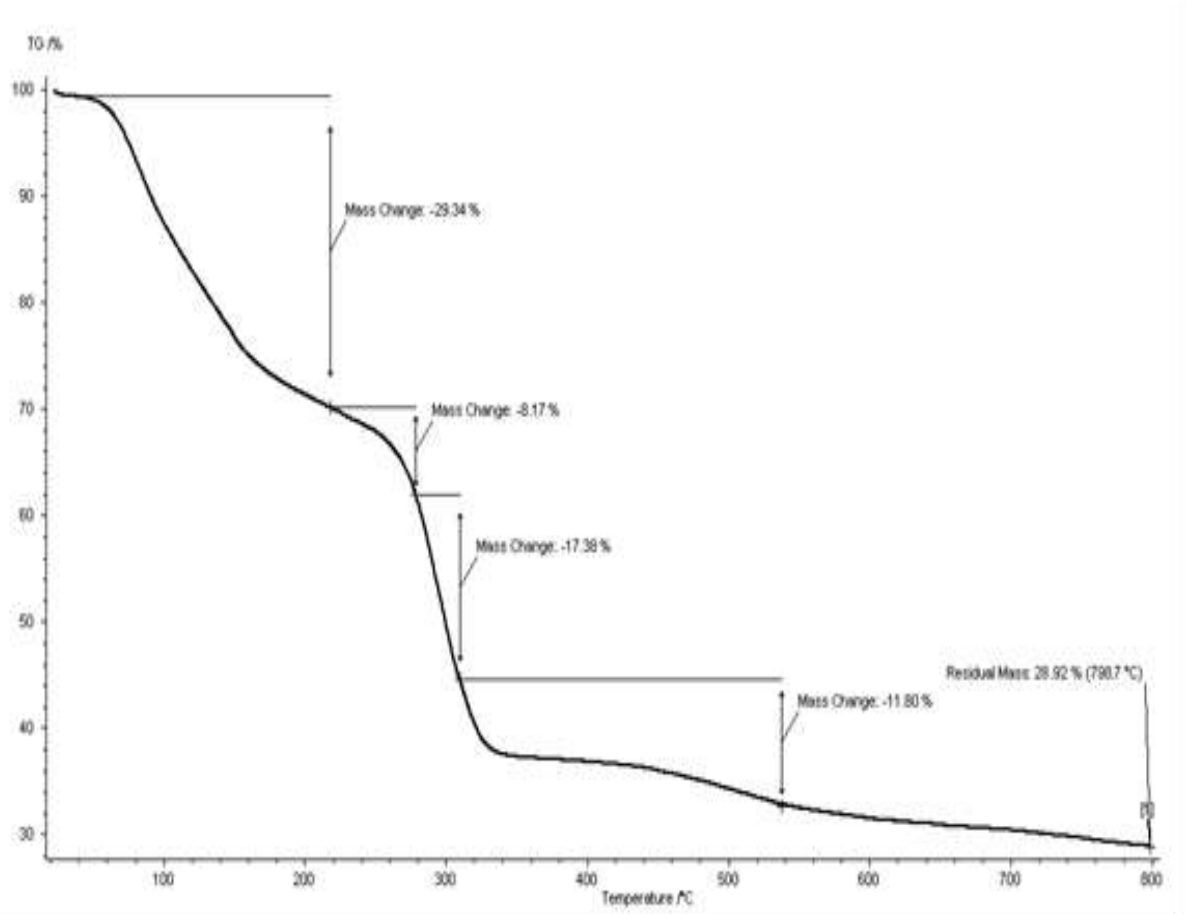

Figure 6: TGA Thermogram Showing Thermal Decomposition Stages of Ethyl Carbamate after Application of the SWPR Using Pd Electrode.

3.7. Mechanisms of CO_2 with Ethanolamine

The application of a square wave potential, cycling between 1.0 V and 0.4 V, is proposed to enhance the CO□ reduction process by facilitating alternating reductive and oxidative steps on the electrode surface, thereby potentially lowering the activation barrier. The mechanism likely involves an initial interaction between dissolved CO□ and the ethanolamine (EA) molecule. Specifically, CO□ reacts with the amine functional group (NH□) of EA, leading to the formation of a zwitterionic intermediate, commonly referred to as carbamic acid (EACOO□), **as depicted in Equation 1**

$CO_2+H_2NCH_2CH_2OH \rightarrow H_2N+CH_2CH_2OCOO^-+H^+$ (Eq. 1)

Under the influence of the SWPR, the palladium electrode surface catalyzes a proton coupled electron transfer (PCET) process involving this zwitterionic intermediate. Bicarbonate (HCO□□) and carbonate (CO□²□) ions, formed from the hydration of CO□, may play a role in stabilizing reaction intermediates. The subsequent step involves the dehydration of the carbamic acid intermediate to yield the final product, ethyl carbamate ($C_2H_5OCONH_2$), **as shown conceptually in Equation 2**

$H_2N+CH_2CH_2OCOO^- \rightarrow C_2H_5OCONH_2+H_2O$ (Eq. 2)

A plausible reaction pathway involves (1) Adsorption of CO□ onto the Pd surface under SWPR conditions; (2) Formation of the zwitterion through the reaction of adsorbed CO□ with ethanolamine; (3) Palladium catalyzed PCET involving the zwitterion (4) Dehydration leading to ethyl carbamate formation. This proposed mechanism centers on the zwitterionic intermediate pathway. The initial reaction between CO□ and the NH□ group of ethanolamine forms the carbamic acid species (EACOO□), potentially stabilized by bicarbonate ions present in the solution. The SWPR applied to the Pd electrode then promotes the crucial PCET step, which ultimately enables the dehydration reaction to form ethyl carbamate.

The alternating potentials inherent in the square wave likely help prevent passivation of the Pd surface, contributing to the observed stable current density (71 mA cm□²). Analytical data from FTIR and MS confirm the high selectivity towards ethyl carbamate, with no significant formation of common competing products like formate or methanol, highlighting the effectiveness of SWPR in directing the reaction pathway. This mechanism aligns with established literature regarding zwitterion formation in CO_2 amine systems [34] and the role of palladium in facilitating PCET reactions [36].

The interaction between CO□ and ethanolamine is influenced by the electrocatalytic properties of the palladium electrode. The SWPR likely enhances the interaction of both CO_2 and EA near the electrode's active sites. Experimental results support the notion that carbamate formation proceeds via the zwitterion mechanism, initiated during the interaction (absorption/adsorption) phase of EA and CO_2 [34]. Further mechanistic considerations suggest that after the initial formation of the carbamic acid species (EACOO□), subsequent reactions involving hydrated CO□ species (HCO_3□/CO_3^{2}□) might occur, potentially leading to carbamate formation through reaction with carbamic acid [35], **as represented generally in Equation 3**

$CO_2 + EA \rightleftharpoons EACOO + HCO_3^- \rightleftharpoons EACOOH$. (Eq. 3)

Regarding performance metrics, current density (j) is a key indicator of the electrochemical reaction rate. It is defined as the measured current (i) divided by the geometric surface area (A) of the working electrode **(Equation 4)**

$$j = i / A \quad \text{(Eq. 4)}$$

Faradaic efficiency (FE) is another critical parameter, quantifying the selectivity of the electrochemical process towards the desired product [36]. It represents the ratio of the charge consumed in forming the target product to the total charge passed during electrolysis. FE can be calculated using Equation 5, where 'a' is the number of electrons transferred per mole of product, 'N' is the number of moles of the desired product formed, 'F' is the Faraday constant (96,485 C mol□¹), and 'Q' is the total charge passed [37]

$$FE = (a * N * F) / Q \quad \text{(Eq. 5)}$$

Table 2: The Summary of Various Materials for Electrochemical CO_2 Reduction. Details Included Faradaic Efficiency, Catalysts, Electrolyte, and Current Density.

No.	Catalyst	Current Density (mA cm^{-2})	Faradaic Efficacy	Electrolyte	Ref.
1	MoS_2	65	98%	H_2O	38
2	TiO_2	68	85%	$KHCO_3$	39
3	Ni	1.45	90%	$KHCO_3$	40
5	Ag_2S	70 µA cm^{-2}	87.4%	HCO_3	41
6	Pd	71	93%	EA	My work

4. CONCLUSION

In summary, this research successfully demonstrates an effective method for synthesizing ethyl carbamate electrochemically from ethanolamine solutions saturated with carbon dioxide, employing a square wave potential regime (SWPR) in conjunction with palladium electrodes. Through optimization of reaction parameters, the process exhibited notable selectivity, achieving a Faradaic efficiency of 93% for ethyl carbamate, alongside stable operation indicated by a current density of 71 mA cm□². The identity and formation of the target product were rigorously confirmed using a combination of spectroscopic (FTIR, UV Vis, NMR, MS) and thermal (TGA) analysis techniques. This investigation contributes to the advancement of CO_2 utilization technologies by effectively coupling CO_2 capture (in ethanolamine) with its subsequent electrochemical conversion, presenting a potentially scalable pathway for producing valuable chemical compounds from CO_2

REFERENCES

I. Hussain, A. Rehman, C. Işık, Using an asymmetrical technique to assess the impacts of CO_2 emissions on agricultural fruits in Pakistan, Environ. Sci. Pollut. Res., 2021, 29, 19378–19389.

A. Goeppert, M. Czaun, J.P. Jones, G.K. Surya Prakash, G.A. Olah, Recycling of carbon dioxide to methanol and derived products–closing the loop, *Chem. Soc. Rev.*, 2014, *43*, 7995 8048.

K. Sonowal, L. Saikia, Metal–organic frameworks and their composites for fuel and chemical production via CO2 conversion and water splitting, *RSC Adv.*, 2022, *12*, 11686–11707.

E. Nikoloudakis, I. López Duarte, G. Charalambidis, K. Ladomenou, M. Ince, A.G. Coutsolelos, Porphyrins and phthalocyanines as biomimetic tools for photocatalytic H2 production and CO2 reduction, *Chem. Soc. Rev.*, 2022, *51*, 6965–7045.

X. Liu, W. Chen, X. Zhang, Highly Active Palladium Decorated Reduced Graphene Oxides for Heterogeneous Catalysis and Electrocatalysis: Hydrogen Production from Formaldehyde and Electrochemical Formaldehyde Detection, N*anomaterials*, 2022, *12*, 1890.

S. Papari, H. Bamdad, F. Berruti, Pyrolytic conversion of plastic waste to value added products and fuels: A review, *Materials*, 2021, *14*, 2586.

H. Park, U. Kang, D. Suk Han, A. Abdel Wahab, Highly Efficient Artificial Photosynthesis of Formate from CO2 and Water on Heterojunction Copper Iron Oxide Catalysts, *Qatar Foundation Annual Research Conference Proceedings*, 2016, 2016:EEPP1751.

Y. Oh, X.L. Hu, *Chem. Organic molecules as mediators and catalysts for photocatalytic and electrocatalytic CO2 reduction, Soc. Rev.*, 2013, *42*, 2253 2261.

C.D. Windle, R.N. Perutz Advances in molecular photocatalytic and electrocatalytic CO2 reduction, *Coord. Chem. Rev.*, 2012, *256*, 2562 2570.

U. Fegade, G. Jethave, Photochemical reduction of carbon dioxide to formic acid, *Green Chemistry*. 2021, 23, 2553 2574.

C.W. Li, M.W. Kanan, CO2 Reduction at Low Overpotential on Cu Electrodes Resulting from the Reduction of Thick Cu2O Films, *J. Am. Chem. Soc.*, 2012, *134*, 7231 7234.

D. Ren, J. Gao, M. Grätzel, Understanding the Electrochemical Reduction of Carbon Dioxide at Copper Surfaces, *ACS Symposium Series*, 2019, *1331*, 209–223.

R. Kortlever, K.H. Tan, Y. Kwon, M.T.M. Koper, Electrochemical carbon dioxide and bicarbonate reduction on copper in weakly alkaline media, *J. Solid State Electrochem.*, 2013, *17*, 1843 1849.

B.C.M. Martindale, R.G. Compton, Formic acid electro synthesis from carbon dioxide in a room temperature ionic liquid, *Chem. Commun.*, 2012, *48*, 6487 6489.

V.S.K. Yadav, M.K. Purkait, Electrochemical reduction of CO 2 to HCOOH on a synthesized Sn electrocatalyst using a Co 3 O 4 anode, *RSC Adv.*, 2015, *5*, 68551 68557.

V.S.K. Yadav, M.K. Purkait, Electrochemical reduction of CO2 to HCOOH using zinc and cobalt oxide as electrocatalysts, *New J. Chem.*, 2015, *39*, 7348 7354.

M. Fan, S. Garbarino, A.C. Tavares, D. Guay, Progress in the electrochemical reduction of CO2 on hierarchical dendritic metal electrodes, *Curr. Opin. Electrochem*, 2020, *23*, 145–153.

H.A. Hansen, J.B. Varley, A.A. Peterson, J.K. Norskov, Understanding Trends in the Electrocatalytic Activity of Metals and Enzymes for CO2 Reduction to CO, *J. Phys. Chem. Lett.*, 2013, *4*, 388–392.

R. Kas, K. Yang, D. Bohra, R. Kortlever, T. Burdyny, W.A. Smith, Electrochemical CO2 reduction on nanostructured metal electrodes: fact or defect?, *Chem. Sci.*, 2020, *11*, 1738 1749.

E.B. Cole, P.S. Lakkaraju, D.M. Rampulla, A.J. Morris, E. Abelev, A.B. Bocarsly, Using a One Electron Shuttle for the Multielectron Reduction of CO2 to Methanol: Kinetic, Mechanistic, and Structural Insights, *J. Am. Chem. Soc.*, 2010, *132*, 11539 11551.

Y.H. Chen, C.W. Li, M.W. Kanan, Aqueous CO_2 Reduction at Very Low Overpotential on Oxide Derived Au Nanoparticles, *J. Am. Chem. Soc.*, 2012, *134*, 19969 19972.

Al Khawaldah, A. Platinum nanoparticle electrode modified iodine used cyclic voltammetry and chronoamperometric for determination of ascorbic acid, Analytical and Bioanalytical Electrochemistry, 2020, 12, 780 792.

M. Hourani, A. Alkawaldeh, Synergistic Effects of Bismuth Adatoms on Electrocatalytic Properties of Electrodeposited Nanostructured Platinum Electrodes, *Int. J. Electrochem. Sci.*, 2016, *11*, 3555–3566.

X. Lu, D.Y.C. Leung, H. Wang, M.K.H. Leung, J. Xuan, Electrochemical reduction of carbon dioxide to formic acid at a tin cathode in divided and undivided cells: effect of carbon dioxide pressure and other operating parameters, *ChemElectroChem*, 2014, *1*, 836 849.

W. Leitner, Carbon Dioxide as a Raw Material: The Synthesis of Formic Acid and Its Derivatives from CO2, *Angew. Chem., Int. Ed. Engl.*, 1995, *34*, 2207 2221.

Y. Hori, H. Wakebe, T. Tsukamoto, O. Koga, Electrocatalytic process of CO selectivity in electrochemical reduction of CO2 at metal electrodes in aqueous media, *Electrochim. Acta*, 1994, *39*, 1833 1839.

N. Furuya, T. Yamazaki, M. Shibata, High performance Ru Pd catalysts for CO2 reduction at gas diffusion electrodes, *J. Electroanal. Chem.*, 1997, *431*, 39 41.

X. Ye, Y. Lu, Kinetics of CO2 absorption into uncatalyzed potassium carbonate–bicarbonate solutions: effects of CO2 loading and ionic strength in the solutions, *Chem. Eng. Sci.*, 2014, *116*, 657–667.

V.S.K. Yadav, M.K. Purkait, Synthesis of Pb_2O electrocatalyst and its application in the electrochemical reduction of CO2 to HCOOH in various electrolytes, *RSC Adv.*, 2015, *5*, 40414 40421.

Al Khawaldah, A. Photocatalytic degradation of platinum nanostructure in tantalum electrode, Journal of Pharmaceutical Negative Results, 2023, 13, 6264–6272.

C. Zhao, Electrochemical reduction of CO2 to formate in aqueous solution using electro deposited Sn catalysts, J. Wang, *Chem. Eng. J.*, 2016, *293*, 161 170.

R.E. Sioda, B. Frankowska, Electro oxidation of alkylnaphthalenes, *J. Electroanal. Chem.*, 2004, 568:365.

B. Lv, B. Guo, Z. Zhou, G. Mechanisms of CO_2 Capture into Monoethanolamine fluid with Different CO2 Loading during the Absorption/Desorption Processes, Jing, *Environ. Sci. Technol.*, 2005, *49*, 10728–10735.

L. Chen, F. Li, Y. Zhang, C. Bentley, M. Horne, A. Bond, J. Zhang, Electrochemical reduction of carbon dioxide in a monoethanolamine capture medium, *Chem.SusChem.*, 2017, *10*, 4109–4118.

J. Rongé, T. Bosserez, D. Martel, C. Nervi, L. Boarino, F. Taulelle, G. Decher, S. Bordiga, J.A. Martens, *Chem. Soc. Rev.*, 2014, *43*, 7963–7981.

Z. Sun, T. Ma, H. Tao, Q. Fan, B. Han, Fundamentals and challenges of electrochemical CO_2 reduction using two dimensional materials, *Chem*, 2017, *3*, 560–587.

M. Asadi, B. Kumar, A. Behranginia, B.A. Rosen, A. Baskin, N. Repnin, D. Pisasale, P. Phillips, W. Zhu, R. Haasch, Robust carbon dioxide reduction on molybdenum disulphide edges, *Nat. Commun.*, 2014, *5*, 4470.

P. Su, K. Iwase, S. Nakanishi, K. Hashimoto, K. Kamiya, Nickel nitrogen modified graphene: an efficient electrocatalyst for the reduction of carbon dioxide to carbon monoxide, *Small*, 2016, *12*, 6083–6089.

W. Bi, X. Li, R. You, M. Chen, R. Yuan, W. Huang, X. Wu, W. Chu, C. Wu, Y. Xie, Surface Immobilization of Transition Metal Ions on Nitrogen Doped Graphene Realizing High Efficient and Selective CO2 Reduction, *Adv. Mater.*, 2018, *30*, 1706617.

C. Zhang, S. Yang, J. Wu, M. Liu, S. Yazdi, M. Ren, J. Sha, J. Zhong, K. Nie, A.S. Jalilov, Electrochemical CO2 Reduction with Atomic Iron Dispersed on Nitrogen Doped Graphene, *Adv. Energy Mater.*, 2018, *8*, 1703487.

H. Li, N. Xiao, M. Hao, X. Song, Y. Wang, Y. Ji, C. Liu, C. Li, Z. Guo, F. Zhang, Efficient CO2 electroreduction over pyridinic N active sites highly exposed on wrinkled porous carbon nanosheets, *Chem. Eng. J.*, 2018, *351*, 613–621.